Unraveling the complexity of flux regulation: A new method demonstrated for nutrient starvation in *Saccharomyces cerevisiae*

Sergio Rossell*, Coen C. van der Weijden*†, Alexander Lindenbergh*, Arjen van Tuijl*, Christof Francke*‡§, Barbara M. Bakker*, and Hans V. Westerhoff*¶‖**

*Faculty of Earth and Life Sciences, Department of Molecular Cell Physiology, Vrije Universiteit Amsterdam, De Boelelaan 1085, 1081 HV, Amsterdam, The Netherlands; ¶Department of Mathematical Biochemistry, BioCentrum Amsterdam, Swammerdam Institute for Life Sciences, Kruislaan 318, 1098 SM, Amsterdam, The Netherlands; ‖Manchester Centre for Integrative Systems Biology, University of Manchester, P.O. Box 88, Sackville Street, Manchester M60 1QD, United Kingdom; and ‡Wageningen Centre for Food Sciences, P.O. Box 557, 6700 AN, Wagenigen, The Netherlands

Communicated by Robert G. Shulman, Yale University, New Haven, CT, November 13, 2005 (received for review April 1, 2005)

An important question is to what extent metabolic fluxes are regulated by gene expression or by metabolic regulation. There are two distinct aspects to this question: (*i*) the local regulation of the fluxes through the individual steps in the pathway and (*ii*) the influence of such local regulation on the pathway's flux. We developed regulation analysis so as to address the former aspect for all steps in a pathway. We demonstrate the method for the issue of how *Saccharomyces cerevisiae* regulates the fluxes through its individual glycolytic and fermentative enzymes when confronted with nutrient starvation. Regulation was dissected quantitatively into (*i*) changes in maximum enzyme activity (V_{max}, called hierarchical regulation) and (*ii*) changes in the interaction of the enzyme with the rest of metabolism (called metabolic regulation). Within a single pathway, the regulation of the fluxes through individual steps varied from fully hierarchical to exclusively metabolic. Existing paradigms of flux regulation (such as single- and multisite modulation and exclusively metabolic regulation) were tested for a complete pathway and falsified for a major pathway in an important model organism. We propose a subtler mechanism of flux regulation, with different roles for different enzymes, i.e., ''leader,'' ''follower,'' or ''conservative,'' the latter attempting to hold back the change in flux. This study makes this subtlety, so typical for biological systems, tractable experimentally and invites reformulation of the questions concerning the drives and constraints governing metabolic flux regulation.

gene expression and metabolic regulation | glycolysis | regulation analysis | metabolic control analysis

The flux through a metabolic pathway is determined by the activities of its enzymes and by their interactions with other enzymes. Metabolic-flux changes have often been observed in response to environmental or genetic changes. In the yeast *Saccharomyces cerevisiae*, for example, changes in glycolytic flux have frequently been found to be accompanied by a myriad of changes in glycolytic enzyme activities (e.g., 1, 2, this work) or amounts (3), which varied in magnitude and direction. The complexity of interactions between enzymes translates into a vast possibility space of combinations of enzyme-activity modulations leading to the same flux change. We wondered how the cell actually regulates its fluxes.

Among the proposed mechanisms for metabolic-flux changes, the two clearest hypotheses are (*i*) modulation of single rate-limiting enzymes and (*ii*) multisite modulation, i.e., simultaneous and proportional modulation of all enzymes in the pathway, thus causing a change in flux while leaving metabolite concentrations unchanged (4). Although single rate-limiting enzymes exist, control of flux is quite often distributed over several enzymes (5). In the latter case, modulation of a single enzyme is likely to be an ineffective mechanism for changing a pathway's flux. Indeed, attempts to correlate flux changes with changes in single enzyme activities or levels have failed consistently (1–3). In contrast, the opposing theory of multisite modulation has met supporting examples, such as lipogenesis in mice, the urea cycle in rats, and photosynthesis in green plants (4). It is not clear, however, how general this mechanism is and whether, indeed, all enzyme activities changed in proportion to the flux.

An important question is to what extent metabolic fluxes are regulated by enzyme capacity (V_{max}) and to what extent by metabolic regulation. According to one paradigm, metabolic fluxes at steady-state are regulated through enzyme-capacity changes (e.g., achieved through changes in gene expression). An orthogonal paradigm has metabolic regulation as dominant. Single- and multisite modulations assume that flux changes are regulated through changes in the capacity of enzymes within the pathway, e.g., through transcription regulation and/or through covalent modification. The single-enzyme-modulation hypothesis does not exclude the possibility of metabolic regulation, but it does assume a leading role of gene expression. In its strongest form, multisite modulation, on the other hand, excludes the possibility of metabolic regulation and proposes metabolite homeostasis as a constraint to regulatory processes. In fact, strong metabolite homeostasis of the glycolytic intermediate glucose-6-phosphate has been demonstrated in rat and human muscle during large changes in glucose consumption, and the mechanism through which metabolite homeostasis was attained has been clearly elucidated (6).

The complexity of interactions and our ignorance of the drives and constraints governing regulatory processes may seem to preclude understanding of flux regulation and to rule out the possibility of testing the above paradigms experimentally. In this article, we demonstrate an unambiguous and quantitative description of regulatory processes that may provide a first step toward understanding them: We use regulation analysis (7, 8) to dissect quantitatively the contributions of changes in maximum enzyme activities (V_{max}) and changes in the interactions of the enzyme with the rest of metabolism to the regulation of fluxes through individual enzymes.

The idea is as follows. Because enzymes are catalysts (and not substrates), enzyme rate equations are usually of the shape

$$v = v(e, \mathbf{X}, \mathbf{K}) = f(\mathrm{e})\cdot g(\mathbf{X}, \mathbf{K}). \quad [1]$$

Conflict of interest statement: No conflicts declared.

Abbreviations: ADH, alcohol dehydrogenase (E.C. 1.1.1.1); ALD, fructose bisphosphate aldolase (E.C. 4.1.2.13); GLT, glucose transporter; HK, hexokinase (E.C. 2.7.1.1); TPI, triosephosphate isomerase, (E.C. 5.3.1.1).

†Present address: DSM Food Specialties, P.O. Box 1, 2600 MA Delft, The Netherlands.

§Present address: Center for Molecular and Biomolecular Informatics, Radboud University Nijmegen, P.O. Box 9010, 6500 GL, Nijmegen, The Netherlands.

**To whom correspondence should be addressed. E-mail: hw@bio.vu.nl.

in which v is the rate, e is the concentration of enzyme, **X** is a vector of concentrations of substrates, products, and other metabolic effectors, and K is a vector of constants parameterizing the strength with which the enzymes interact with their substrates, products, and allosteric effectors. The important characteristic of the above equation is that the multipliers are cross-independent, meaning that f does not depend on **X** and **K**, and g does not depend on e. Exceptions to this equation exist, for instance in some cases of strong substrate channeling. $f(e)$ describes the dependency of the rate on the enzyme concentration and can be taken to equal V_{max}, whereas $g(\mathbf{X}, \mathbf{K})$ describes the interaction of the enzyme with the rest of metabolism through metabolite concentrations and the corresponding affinity constants.

The dissection and quantification of f and g is achieved by translating the above equation into logarithmic space, considering a change between two steady states, and dividing both sides of the equation by the relative change in steady-state flux J. Because at steady state, the flux J equals the enzyme rate v, this results in

$$1 = \frac{\Delta \log f(\mathrm{e})}{\Delta \log J} + \frac{\Delta \log g(\mathbf{X}, \mathbf{K})}{\Delta \log J} = \rho_h + \rho_m. \qquad [2]$$

ρ_h is the "hierarchical regulation coefficient," quantifying the relative contribution of changes in active enzyme concentration to the regulation of the enzyme's flux. ρ_m is the "metabolic regulation coefficient," quantifying the relative contribution of changes in the interaction of the enzyme with the rest of metabolism to the regulation of the enzyme's flux. For a more elaborate description and discussion of the method, see ref. 8. The term hierarchical regulation coefficient was introduced by Ter Kuile and Westerhoff (7) because the V_{max} depends on the complete gene-expression cascade of transcription, translation, posttranslational modification, and mRNA and protein degradation. The two regulation coefficients sum up to one (summation theorem for the regulation of flux), implying that determination of one will yield the other automatically (7, 8). In practice, the hierarchical regulation coefficient is more readily determined, because $f(e)$ can usually be taken to equal V_{max}, and the V_{max} and the flux J through the enzyme can be measured or estimated in most cases. Regulation analysis introduces the possibility of making unambiguous and quantitative descriptions of the regulation of fluxes through individual enzymes embedded in biochemical networks of any complexity, in response to any number or kind of simultaneous perturbations.

In this study, regulation analysis is applied to the regulation of the flux through individual glycolytic and fermentative enzymes in *S. cerevisiae* during nutrient starvation. Starvation for nutrients is perhaps one of the most common stress conditions experienced by microorganisms in their natural habitat, and it may affect most of the organisms' life spans. Nutrient starvation is also relevant for the industrial production of baker's yeast. At the final stages of production and during storage, cells are starved, affecting several quality parameters, among which is the fermentative capacity (3, 9) (the specific rate of CO_2 production under anaerobic conditions with excess of sugar, which almost equals the rate of ethanol formation) (2).

Using regulation analysis, we here dissect quantitatively the regulation of fluxes through individual glycolytic and fermentative enzymes in response to nutrient starvation. Our experimental results served to test three regulatory paradigms (i.e., single enzyme, multisite, and all metabolic). The results evidence a more subtle regulation of cell function and show that this method allows delineating experimentally the regulation of flux. Our results suggest that different enzymes in a common pathway play different roles in the regulation of the pathway's flux.

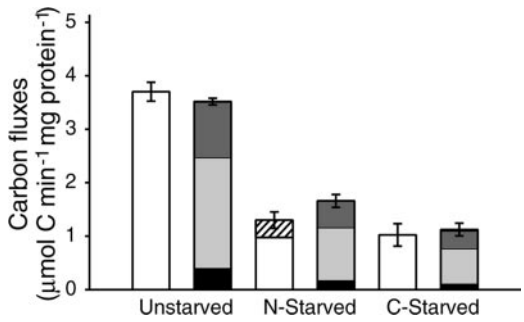

Fig. 2. Carbon-flux balances. The carbon fluxes for each condition are represented with two columns: one depicting the consumed carbon (open columns) and the other the produced carbon (dark shaded areas). Columns are divided into fluxes: glucose (open columns), storage carbohydrates (diagonally striped area), glycerol (black areas), ethanol (light shaded columns), and CO_2 (calculated from the ethanol and acetate production) (dark shaded areas). Error bars represent SEMs of the sum of consumed or produced carbon fluxes of four independent experiments carried out with different batches of cells. Glycogen was measured in only two of the experiments; the average was used as the glycogen-degradation rate of the other two, in which glycogen was not measured.

Results

Steady-State Fluxes. We first measured the overall steady-state fluxes of glucose, ethanol, glycerol, acetate, succinate, glycogen, and trehalose under standardized conditions of growth and starvation. Subsequently, these data were used to calculate the intracellular fluxes through the individual enzymes. *S. cerevisiae* CEN.PK 113–7D was grown in a well aerated and pH-controlled batch culture. An aliquot of cells was harvested during exponential growth and split into three parts. One part (referred to as unstarved) was washed and transferred to an anaerobic vessel with a fresh and complete medium with excess of glucose (101 mM). This condition was meant to mimic the situation of baker's yeast in dough (2). The above-mentioned fluxes were then measured over a period of 30 min. The other two batches of cells were washed and transferred to fresh medium, lacking either ammonium (nitrogen-starved cells) or glucose (carbon-starved cells). After 24 h, the starved cells were harvested, and the fluxes were measured in a complete medium in the same way as was done for the unstarved cells.

Fig. 2 and Table 1 show the measured fluxes. In all conditions, the consumed carbon matched the produced carbon within experimental error. The production fluxes of acetate and succinate were always <1% of the rate of glucose consumption (data not shown). Nitrogen starvation and carbon starvation resulted in a significant and substantial decrease of both the consumption of glucose and the production of ethanol and glycerol under the abundance conditions of the steady-state

Table 1. Measured fluxes

Metabolite	Unstarved	Nitrogen-starved	Carbon-starved
Glucose	−0.62 ± 0.03	−0.16 ± 0.02	−0.17 ± 0.03
Glycerol	0.13 ± 0.01	0.06 ± 0.01	0.04 ± 0.00
Ethanol	1.04 ± 0.03	0.49 ± 0.05	0.33 ± 0.05
Trehalose	0.00 ± 0.00	−0.01 ± 0.00	0.00 ± 0.00
Glycogen	0.00 ± 0.00	−0.03 ± 0.01	0.00 ± 0.00

Experimentally measured fluxes are reported in μmol of the compound per minute per mg of protein for each condition. Negative values represent fluxes feeding the pathway, and positive values represent outgoing fluxes. Errors are SEM for four independent experiments carried out with different batches of cells, except for glycogen. Glycogen errors are SD for two independent experiments carried out with different batches of cells.

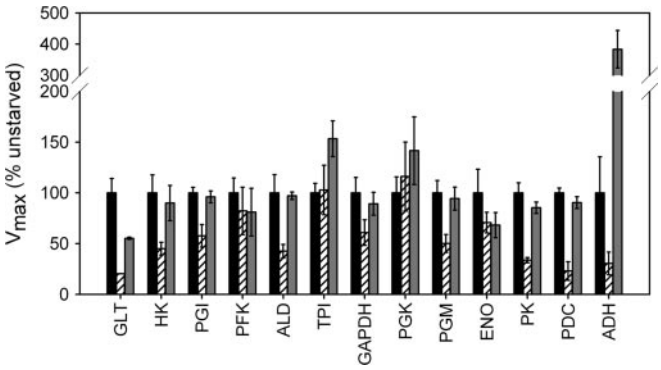

Fig. 3. V_{max} values as a percentage of those in unstarved cells. The percentage of V_{max} values with respect to the unstarved condition of glycolytic and fermentative enzymes and of the GLT are shown: unstarved (black columns), nitrogen-starved (diagonally striped columns), and carbon starved (gray columns). Error bars of glycolytic and fermentative enzymes represent the percentage SEM, with respect to their corresponding unstarved mean V_{max} value, of four independent experiments carried out on different batches of cells. Error bars of the GLT represent the percentage SD, with respect to the unstarved mean V_{max} value, of two independent experiments carried out on different batches of cells.

measurements assay (Student's t test, $\alpha = 5\%$). During the starvation period, nitrogen-starved cells accumulated trehalose and glycogen. Upon transfer to complete medium, these storage carbohydrates were degraded, fueling glycolysis and contributing to the production of ethanol and glycerol.

The measured steady-state fluxes of ethanol, glycerol, and glucose were used to calculate fluxes through individual enzymes in the manner detailed in *Materials and Methods*. Fig. 1 shows the resulting fluxes of nitrogen- (underlined) and carbon-starved cultures as a percentage of those in unstarved cultures. Nutrient starvation resulted in a substantial down-regulation of the fluxes through all glycolytic and fermentative enzymes, up to >70% in the case of the GLTs.

Enzyme Activities. Next, we asked to what extent the observed decrease of the fluxes through the glycolytic enzymes was regulated through changes of their maximum activities (V_{max}). Therefore, we measured the maximum enzyme activities in unstarved cells and after 24 h of nitrogen or carbon starvation.

Nutrient starvation resulted in changes of V_{max} that varied in extent and direction (Fig. 3). The cells responded in a very different way to the two types of starvation. During nitrogen starvation, the activities of GLT, HK, glucose-6-phosphate isomerase, ALD, phosphoglycerate mutase, pyruvate kinase, pyruvate decarboxylase, and alcohol dehydrogenase (ADH) were down-regulated (Student's t test $\alpha = 5\%$), whereas the other enzyme activities remained unchanged within statistical error. During carbon starvation, on the other hand, only the V_{max} of the GLT decreased significantly, whereas the maximum activities of TPI and ADH increased (Student's t test $\alpha = 5\%$).

Regulation Analysis. Nutrient starvation resulted in decreased fluxes and a variety of V_{max} changes. To dissect the extent to which the changes of V_{max} were responsible for the flux changes from the extent to which the fluxes were, rather, regulated by changes in their interaction with the rest of metabolism, we calculated the hierarchical and metabolic regulation coefficients (see Eqs. **2** and **3**). The results are shown in Table 2. The hierarchical regulation coefficients, ρ_h, ranged between −1.3 and 2.2, spanning all categories of regulation (8). This wide variation of ρ_h is not a matter of statistical variation (see Table 2).

We distinguish the following categories of regulation:

Table 2. Hierarchical and metabolic regulation coefficients of nitrogen and carbon starvations

	Nitrogen starvation			Carbon starvation		
Enzyme	ρ_h	SEM	ρ_m	ρ_h	SEM	ρ_m
GLT	1.2	0.1	−0.2	0.4	0.1	0.6
HK	1.0	0.2	0.0	0.1	0.0	0.9
PGI	0.8	0.3	0.2	0.0	0.0	1.0
PFK	0.4	0.2	0.6	0.4	0.4	0.6
ALD	1.1	0.5	−0.1	0.0	0.2	1.0
TPI	0.1	0.9	0.9	−0.4	0.2	1.4
GAPDH	0.7	0.5	0.3	0.1	0.0	0.9
PGK	0.0	0.2	1.0	−0.3	0.1	1.3
PGM	1.0	0.4	0.0	0.0	0.0	1.0
ENO	0.4	0.5	0.6	0.3	0.1	0.7
PK	1.4	0.3	−0.4	0.1	0.0	0.9
PDC	2.3	0.6	−1.3	0.1	0.0	0.9
ADH	1.7	0.4	−0.7	−1.3	0.2	2.3

PDC, pyruvate decarboxylase; PFK, 6-phosphofructokinase; PGI, glucose-6-phosphate isomerase; PGK, phosphoglycerate kinase; PGM, phosphoglycerate mutase; PK, pyruvate kinase; TPI, triose-phosphate isomerase.

Purely hierarchical regulation. During nitrogen starvation, the hierarchical regulation coefficient (ρ_h) of a number of enzymes was not significantly different from 1. Because the metabolic and the hierarchical regulation coefficients sum up to 1 (Eq. **1**), these enzymes had a metabolic regulation coefficient (ρ_m) not significantly different from 0, implying that the change of flux was regulated predominantly by the change in V_{max}, whereas the interaction with the rest of metabolism made a negligible contribution. HK and phosphoglycerate mutase were the clearest examples of this type of regulation.

Purely metabolic regulation. Enzymes with ρ_h not significantly different from 0 were found in both types of starvation. For these enzymes, the flux was predominantly regulated by the interaction with the rest of metabolism without any significant contribution of changes in V_{max}. PGK in nitrogen starvation, and glucose-6-phosphate isomerase, ALD, and phosphoglycerate mutase in carbon starvation were the clearest examples of this category.

Cooperative regulation. A number of enzymes were regulated cooperatively by changes in V_{max} and changes in their interaction with the rest of metabolism, reflected by a ρ_h value between 0 and 1 and significantly different from both 0 and 1. Six-phosphofructokinase was regulated in this way during nitrogen starvation and so were GLT and ENO during carbon starvation.

Antagonistic regulation directed by metabolism. Negative ρ_h values result when the flux changes in opposite direction to the V_{max}. In these cases, ρ_m was >1, implying that the metabolic regulation dominated and was counteracted by hierarchical regulation, which acted "conservatively," in that it attempted to antagonize the flux change. The regulation of ADH during carbon starvation was an outstanding instance of this category.

Antagonistic regulation directed by V_{max}. This category is the opposite of the previous. ρ_h exceeded 1, and ρ_m was therefore negative. In these cases, the changes in the interaction with the rest of metabolism and the changes of V_{max} again counteracted each other, but now the change of V_{max} dominated the outcome, with the metabolic regulation acting conservatively. Only nitrogen starvation showed enzyme fluxes regulated in this way. PDC and ADH were the most conspicuous cases. Also, GLT was classified in this category, but it should be noticed that its ρ_h was very close to 1, meaning that its regulation was predominantly hierarchical, with a small, but significant, antagonistic contribution of the interaction with the rest of metabolism.

Discussion

Nutrient starvation of the yeast *S. cerevisiae* resulted in decreased glucose consumption and decreased ethanol and glycerol production (3, 9, 10, this study). These flux decreases were accompanied by a limited variety of changes in the maximum activities of glycolytic and fermentative enzymes. The changes differed in magnitude and direction among enzymes, and the profile of these changes differed between starvation types (3, 10). Similar findings have been reported for other transitions, such as changes of dilution rates in chemostat cultures (2) or shifts between different growth limitations (1).

Our goal was to understand the regulation of metabolic fluxes by the concerted action of gene expression and metabolic interactions. There are two related but different aspects to this problem. On the one hand, there is the local regulation of fluxes through individual enzymes, and, on the other hand, there is the extent to which this local regulation influences the pathway's (global) flux. In this contribution, we expound on how the first aspect can be understood. Using regulation analysis, we determined experimentally the type of regulation of fluxes through individual glycolytic and fermentative enzymes, as yeast was responding to nutrient starvation. We and others have applied this method to the regulation of flux through some steps in a pathway (7, 8, 11). This article reports a comprehensive study extending regulation analysis to all enzymes in a complete metabolic pathway so that we could address the validity of a number of existing paradigms of metabolic regulation of pathway flux.

In the introduction, we distinguished three regulatory paradigms, i.e., single enzyme, multisite, or all metabolic. If we translate these paradigms to the terminology of regulation analysis, single-enzyme regulation implies that one enzyme is regulated in a purely hierarchical manner ($\rho_h = 1$), whereas all of the others are regulated only through metabolism ($\rho_h = 0$). Neither our results nor those of others are compatible with single-enzyme regulation (1–3, 10).

The hypothesis of multisite modulation proposes metabolite homeostasis as a constraint to metabolic-flux regulation, excluding the possibility of metabolic regulation, corresponding to a situation where $\rho_h = 1$ for all enzymes. In our carbon-starvation experiments, however, a number of fluxes through individual enzymes were regulated exclusively by the interaction of the enzyme with the rest of metabolism ($\rho_h = 0$). Among these enzymes, glucose-6-phosphate isomerase and ALD have a unique isoenzyme form, excluding that this apparent metabolic regulation is actually caused by K_m changes through the expression of isoenzymes. During nitrogen starvation, unspecific degradation of proteins via autophagy is enhanced (12), and, therefore, one might have expected a proportional decrease of all enzyme amounts (corresponding to multisite modulation). We observed, however, disproportional changes in enzyme activities (ρ_hs unequal to each other and $\neq 1$). Protein degradation is, therefore, unlikely to be the sole cause of these enzyme-activity changes.

The third paradigm, exclusively metabolic regulation, would correspond to all $\rho_h = 0$. Our results are incompatible with this hypothesis.

If none of these three regulatory paradigms holds true, how should we then envisage regulation? Within a single pathway, fluxes through individual enzymes were regulated in different ways, suggesting that enzymes play different roles in the regulation of the pathway's flux. Changes in fluxes through some enzymes were caused predominantly by changes in enzyme activities ($\rho_h \approx$ or > 1). The interaction with the rest of metabolism either complied ($\rho_m = 0$) or antagonized, diminishing the effect of the enzyme activity change on the local flux ($\rho_m < 0$). In these cases, enzyme-activity changes seemed to "lead" the regulatory response, whereas the compliance or antagonism of the interaction with the rest of metabolism constituted the system's response to this lead. Other enzyme fluxes were regulated with small or no change in enzyme activities ($0 < \rho_h \ll 1$ and $\rho_h = 0$, respectively). These enzymes seemed to "follow" the leader enzymes by adjusting their rate through their interaction with the rest of metabolism. Yet, other enzymes changed their maximum activity in opposite direction to the change in flux ($\rho_h < 0$). These "conservative" enzymes seemed to "pull back," to restrain the regulation by the leading enzymes. Interestingly, the pathway's regulation profile differed radically between the two types of starvation. The sets of enzymes leading the regulatory response, as well as those following or pulling back, differed between starvation types. Apparently, the regulatory roles of enzymes are not fixed properties but, rather, change when cells are challenged in different ways. And this finding is what we should like to propose as a paradigm for metabolic regulation: Regulation is diverse within a pathway, some enzymes taking the lead, others helping, and yet others acting conservatively.

Several experimental limitations constrain further conclusions from and, indeed, the accuracy of, our analysis. First, some of the calculated regulation coefficients presented in Table 2 have relatively high SEMs, due to the necessary (because we are studying regulation) consideration of changes of fluxes and enzyme activities instead of absolute values in their calculation. The large errors limit the application of regulation analysis to the analysis of perturbations that cause relatively large changes of flux and stresses on the necessity to further develop the reproducibility of analytical techniques and of cultivation and sampling procedures. However, the large errors do not impede an unambiguous classification of most enzymes in different regulation categories, proving that these classifications are not just theoretical possibilities, but actual ways by which living cells regulate fluxes through individual enzymes. And here, regulation analysis differs from metabolic control analysis, in that regulation analysis does not require changes to be small.

Another crucial issue is a correct estimation of the local fluxes. Based on measured fluxes (Table 1), we calculated the fluxes through individual glycolytic and fermentative enzymes by using the simplified scheme depicted in Fig. 1. We neglected the branching fluxes through the pentose phosphate pathway and through the anabolic pathways. Although the differences between produced and consumed carbon are not statistically significant (Fig. 2), mean consumed carbon was in excess with respect to produced carbon in unstarved cultures, whereas the reverse was suggested for starved cultures. Because absolute growth during our 30-min assay is undetectable, we estimated the fraction of glycolytic flux diverged into biomass. Because the biomass yield for optimal anaerobic growth is 0.1 g of biomass per g of glucose, and the carbon content of biomass is 40% (13), 10%, at most, of the glucose may be incorporated into biomass. Because *S. cerevisiae* lacks a transhydrogenase, the pools of NADPH and NADH are not linked (14). For each mole of glucose going into biomass, 1 mole of NADPH is required (15). If 10% of the glucose is used for biomass production, then, at most, 5% of the glucose flows through the phosphogluconate pathway (two NADPH are produced per glucose 6-phosphate rerouted). Based on these calculations, we neglected the branches into the pentose phosphate pathway and into anabolism: Taking them into account would not change our regulation coefficients such that our above conclusions would change.

Another simplification in Fig. 1 was the exclusion of fructose-1,6-bisphosphatase. This enzyme may cause substantial futile cycling, particularly in the transition from carbon-starved media to complete media (16). However, in our experimental conditions, the activity of fructose-1,6-bisphosphatase was very low in all cultures (<0.002 μmol·min^{-1}·mg of protein^{-1}). In contrast to ref. 16, our starved cells were not adapted to growth on acetate or another gluconeogenic substrate: The required stimuli for

triggering the expression of fructose-1,6-bisphosphatase may have been absent under our experimental conditions.

It is possible to extend regulation analysis to further dissect the different processes within the hierarchical component (17). In a pilot experiment, we investigated whether any change in V_{max} occurred at 15 min after the transfer of starved cells into complete medium, the timescale at which covalent modifications may occur. The changes in V_{max} we measured were not beyond what was to be expected on the basis of statistical variation, with the exception of pyruvate kinase (PK). We observed an activation of PK in nitrogen- and carbon-starved cultures, 6- and 16-fold, respectively (result not shown). Indeed, PK has been reported to be activated through phosphorylation by protein kinase A (18).

Concerning the regulation of the pathway's flux, our results suggest that changes outside glycolysis contributed to the decrease of glycolytic flux in carbon-starved cells, regulating glycolytic enzymes metabolically. The only V_{max} that decreased significantly was that of the GLT. However, the decrease of the transporter V_{max} was only 40% of the decrease of the flux. The remaining 60% of metabolic regulation is unlikely to be initiated by any of the other enzymes in the pathway, because no other V_{max} decreased significantly. Thus, part of the metabolic regulation of glycolytic and fermentative enzymes during carbon starvation must have originated outside the pathway. We measured the concentrations of two obvious candidates, ATP and ADP (data not shown). Their ratio did not change (0.7), but changes in the total concentration of the summed adenine nucleotides (ATP + ADP + AMP) may still be involved in the decrease of glycolytic flux.

Our results and analysis have shown that pathway fluxes may be regulated not only through expression of enzymes within the pathway but also through metabolic regulation that may be elicited by changes foreign to the pathway in study. Thus, our findings highlight the need to integrate transcriptome and proteome analyses with other levels of regulation, including the metabolic and to do so quantitatively. Using regulation analysis, we have described the regulation of steady-state fluxes through individual enzymes, unraveling a previously undescribed complexity of flux regulation. The diversity of regulation within a common pathway suggests that enzymes play a limited number of different regulatory roles. We suggest an alternative mechanism for flux modulation, a mechanism in which regulation is not exclusively hierarchical, as in multisite modulation, nor effected by a single regulatory enzyme but involves different regulatory roles for each enzyme and a plasticity that allows these roles to shift between enzymes when the cell is confronted with different challenges. Our findings invite us to reconsider our views on regulatory processes. Regulation of metabolic fluxes needs not be governed by single drives or constraints but may result from a combination of the two, and their relative importance may well vary between challenges.

Materials and Methods

Growth and Starvations. The growth and starvation procedures have been described in detail in ref. 8. Briefly, *S. cerevisiae* strain CEN-PK 113–7D (*MATa MAL2–8^c SUC2*) was grown in pH-controlled batch cultures at 30°C in defined mineral medium containing 101 mM glucose (19) kept at pH 5.0. Cells were harvested by centrifugation at an $OD_{600\ nm}$ of 1.0 (exponential phase). For starvation experiments, the pellets were washed with equal volumes of ice-cold growth medium lacking either glucose or ammonium and resuspended in the corresponding medium to a cell density of 0.75% wet weight (≈1g dry weight l^{-1}) at pH 6.0. The suspensions, of ≈300 ml, were kept in 2-liter shake flasks on a rotary shaker at 30°C and 200 rpm without pH control for 24 h. For the measurement of steady-state fluxes, the cells were harvested by centrifugation, resuspended in growth medium without a carbon source, and kept on ice for, at most, 1 h. Similarly, for the measurement of zero-trans influx of glucose, cells were harvested by centrifugation, resuspended in growth medium lacking carbon and nitrogen sources, and kept on ice for, at most, 1 h.

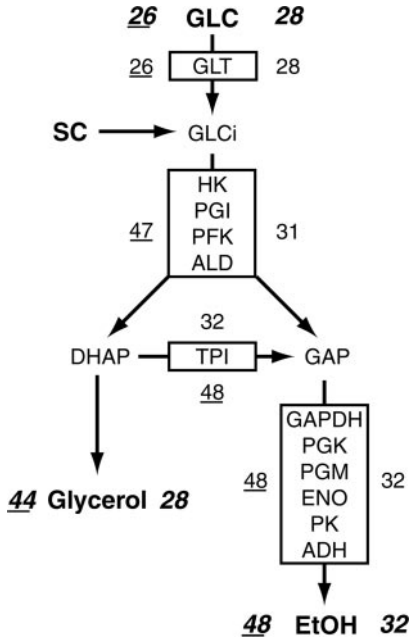

Fig. 1. Stoichiometry of the glycolytic and fermentative pathways. In this simplified scheme of the glycolytic and fermentative pathways, enzymes are boxed, and those with the same flux are boxed together. Measured fluxes are depicted in boldface letters, and branching metabolites connect the boxes. Numbers represent the flux percentages of starved cultures with respect to the unstarved condition. Underlined numbers are the percentage flux of nitrogen-starved cultures, and numbers without underline are the corresponding percentages for carbon-starved cultures. Measured fluxes are distinguished from calculated fluxes by being represented in boldface letters. GLC, glucose flux; SC, steady-state degradation of storage carbohydrates; EtOH, ethanol flux; DHAP, dihydroxyacetonephosphate; GAP, glyceraldehyde-3-phosphate, GLCi, intracellular glucose; SC, storage carbohydrates. Enzyme abbreviations are in the main text.

Steady-State Fluxes. Steady-state fluxes were measured for 30 min in a cell suspension kept anaerobic at 30°C in a setup described by Van Hoek *et al.* (2) for the determination of fermentative capacity, with the modification that the headspace was flushed with N_2 instead of CO_2. Ethanol, glucose, glycerol, succinate, acetate, and trehalose were measured by HPLC (300 mm × 7.8 mm ion exchange column Aminex-HPX 87H (Bio-Rad), with 22.5 mM H_2SO_4 kept at 55°C as eluent at the flow rate of 0.5 ml·min^{-1}). Glycogen was assayed according to Parrou and Francois (20). The rate of carbon dioxide production was calculated from the production rates of ethanol and acetate.

The flux through the glucose transporter (GLT) was taken as equal to the measured glucose consumption flux. The fluxes through enzymes downstream hexokinase (HK) were calculated from the steady-state rates of ethanol and glycerol production. Fig. 1 shows a scheme of the pathway. Enzymes with the same flux are boxed together. The flux through HK, glucose-6-phosphate isomerase, 6-phosphofructokinase, and aldolase (ALD) was calculated by dividing the sum of the glycerol and ethanol fluxes by two. The flux through triose-phosphate isomerase (TPI) was calculated by subtracting the rate of glycerol from the flux through the previous block (HK until ALD), and the flux

through the enzymes downstream GAPDH was taken as equal to the measured ethanol flux.

Glucose-Transport Activity Measurements. Zero-trans influx (the initial rate of transport before the product, intracellular glucose, builds up) of ^{14}C radiolabeled glucose was measured in a 5-second uptake assay at 30°C according to Walsh *et al.* (21), with the modifications introduced by Rossell *et al.* (8). The range of glucose concentrations was between 0.25 and 225 mM. Irreversible Michaelis–Menten equations were fitted to the results by nonlinear regressing by using SIGMAPLOT 2001 version. 7.0 (SPSS).

Enzyme-Activity Measurements. Enzyme extracts were prepared by sonication with glass beads at 0°C as described by van Hoek *et al.* (2). Enzyme activity assays were carried out on four dilutions of freshly prepared extracts through NAD(P)H-linked assays as described by van Hoek *et al.* (2), by using a Cobas Bio (Roche) automated analyzer for spectroscopic measurements. As a control, an extraction was done in the presence and in the absence of phosphatase inhibitors (10 mM sodium fluoride and 5 mM sodium pyrophosphate), and V_{max} changes were small and within the expected statistical variation.

Regulation Analysis. Hierarchical regulation coefficients (ρ_h) were calculated as follows:

$$\rho_h = \frac{\log V_{\text{max\_starved}} - \log V_{\text{max\_unstarved}}}{\log J_{\text{starved}} - \log J_{\text{unstarved}}}, \qquad [3]$$

where the subscripts "starved" and "unstarved" refer to starved (for nitrogen or carbon) or unstarved cell suspensions, respectively. Each starvation experiment provided three cell suspensions, one for each condition. We performed four independent starvation experiments to measure V_{max} values and another four to estimate fluxes through individual enzymes. The numerator of Eq. **3** was calculated for each starvation experiment, the values were averaged, and their SD was computed. The average and SD of the denominator was computed in the same way. Dividing average numerator and denominator yielded the average ρ_h. The metabolic regulation coefficient was calculated by subtracting ρ_h from 1.

We thank J. T. Pronk, P. Daran-Lapujade, K. van Dam, and M. J. Teixeira de Mattos for invaluable discussions and the anonymous reviewers for their comments. This work was supported by Netherlands Technology Foundation Grant DGC 5232 and BioSim NoE Grant FP6-EU.

1. Daran-Lapujade, P., Jansen, M. L., Daran, J. M., van Gulik, W., de Winde, J. H. & Pronk, J. T. (2004) *J. Biol. Chem.* **279,** 9125–9138.
2. Van Hoek, P., Van Dijken, J. P. & Pronk, J. T. (1998) *Appl. Environ. Microbiol.* **64,** 4226–4233.
3. Nilsson, A., Pahlman, I. L., Jovall, P. A., Blomberg, A., Larsson, C. & Gustafsson, L. (2001) *Yeast* **18,** 1371–1381.
4. Fell, D. A. & Thomas, S. (1995) *Biochem. J.* **311,** 35–39.
5. Fell, D. A. (1992) *Biochem. J.* **286,** 313–330.
6. Shulman, R. G., Bloch, G. & Rothman, D. L. (1995) *Proc. Natl. Acad. Sci. USA* **92,** 8535–8542.
7. ter Kuile, B. H. & Westerhoff, H. V. (2001) *FEBS Lett.* **500,** 169–171.
8. Rossell, S., van der Weijden, C. C., Kruckeberg, A. L., Bakker, B. M. & Westerhoff, H. V. (2005) *FEMS Yeast Res.* **5,** 611–619.
9. Rossell, S., van der Weijden, C. C., Kruckeberg, A., Bakker, B. M. & Westerhoff, H. V. (2002) *Mol. Biol. Rep.* **29,** 255–257.
10. Thomsson, E., Larsson, C., Albers, E., Nilsson, A., Franzen, C. J. & Gustafsson, L. (2003) *Appl. Environ. Microbiol.* **69,** 3251–3257.
11. Even, S., Lindley, N. D. & Cocaign-Bousquet, M. (2003) *Microbiology* **149,** 1935–1944.
12. Abeliovich, H. & Klionsky, D. J. (2001) *Microbiol. Mol. Biol. Rev.* **65,** 463–479.
13. Verduyn, C., Stouthamer, A. H., Scheffers, W. A. & van Dijken, J. P. (1991) *Antonie Leeuwenhoek* **59,** 49–63.
14. Bakker, B. M., Overkamp, K. M., van Maris, A. J., Kotter, P., Luttik, M. A., van Dijken, J. P. & Pronk, J. T. (2001) *FEMS Microbiol. Rev.* **25,** 15–37.
15. Verduyn, C., Postma, E., Scheffers, W. A. & van Dijken, J. P. (1990) *J. Gen. Microbiol.* **136,** 395–403.
16. Shulman, R. G. & den Hollander, J. (2004) in *Metabolomics by in Vivo NMR*, eds. Shulman, R. G. & Rothman, D. L. (Wiley, New York), pp. 206.
17. Westerhoff, H. V., Reijenga, K. A., Snoep, J. L., Kholodenko, B. N. & ter Kuile, B. H. (2000) in *Animating the Cellular Map*, eds. Hofmeyr, J. H. S., Rohwer, J. M. & Snoep, J. L. (Stellenbosch Univ. Press, Stellenbosch, South Africa), pp. 1–7.
18. Portela, P., Howell, S., Moreno, S. & Rossi, S. (2002) *J. Biol. Chem.* **277,** 30477–30487.
19. Verduyn, C., Postma, E., Scheffers, W. A. & Van Dijken, J. P. (1992) *Yeast* **8,** 501–517.
20. Parrou, J. L. & Francois, J. (1997) *Anal. Biochem.* **248,** 186–188.
21. Walsh, M. C., Smits, H. P., Scholte, M. & van Dam, K. (1994) *J Bacteriol.* **176,** 953–958.